Electronic Supplementary Material (ESI) for RSC Advances.

Electronic Supplementary Information

Cysteine-based fluorescence "turn-on" sensors for $Cu^{2+}$and Ag^{+}

V. Haridas,[†] P. P. Praveen Kumar,[†] and Cherumuttathu H. Suresh[‡]

[†] *Department of Chemistry, Indian Institute of Technology Delhi, New Delhi -110016, India, and*

[‡]*Computational Modeling and Simulation, National Institute for Interdisciplinary Science and Technology, (NIIST-CSIR) Thiruvananthapuram–695019, India.*

Experimental section

General experimental:

All reagents were used without further purification. All solvents employed in the reactions were distilled and dried from appropriate drying agents prior to use. Progress of reactions was monitored by silica gel thin layer chromatography (TLC). Purification of compounds was done by silica gel column chromatography. Silica gel G (Merck) was used for TLC and silica gels with 60-120 mesh used for column chromatography. Melting points were recorded on a Fisher-Scientific melting point apparatus and were uncorrected. IR spectra were recorded on a Nicolet, Protégé 460 spectrometer as KBr pellets. ^{1}H NMR spectra were recorded on Brucker-DPX-300 spectrometer using tetramethylsilane (^{1}H) as an internal standard. Coupling constants are in Hz and the ^{1}H NMR data are reported as s (singlet), d (doublet), br (broad), t (triplet) and m (multiplet), dd (double doublet). High resolution mass spectra (HRMS) was recorded on AB Sciex, 1011273/A model using ESI-technniqe. UV-Visible spectra were recorded in Shimadzu double beam spectrophotometer, UV-2400. The emission spectra were recorded in HORIBA JOBIN YVON Scientific, fluoromax - 4 spectrofluorometer with slit width of 5 nm. Life-time measurements were conducted in IBH-Time correlated Single Photon Counting System with slit width 5 nm. The thermodynamic parameters were estimated by MicroCal iTC$_{200}$ system at 298K in acetonitrile. The nonlinear least square algorithm and the concentration of the sample solution was used to determine the best fit values of change in enthalpy (ΔH), change in entropy (ΔS) and binding constant (K).

Preparation of 1

To L-Cysteine (121 mg, 1 mmol), tertiary butanol (0.13 mL, 1.3 mmol) was added and mixed throughly. To this 2N HCl (0.40 mL, 0.013 mmol) was added and reaction mixture was refluxed for 12 h at 110°C. The reaction mixture was concentrated under reduced pressure and crystalline product was filtered off, washed with dry acetone.

%Yield: 84%

m.p : 200-202°C

^{1}H NMR (D_2O, 300 MHz) δ: 1.20 (s, 9H), 3.01 (br d, 2H), 3.92 (m, 1H)

^{13}C NMR (D_2O,75 MHz) δ: 26.4, 32.5, 42.1, 56.8, 172.3

IR (KBr): 3390, 2992 (br), 1742, 1625, 1571, 1520 (br), 1428, 1400, 1347, 1274, 1220, 1200 cm^{-1}.

HRMS : Calculated for $C_7H_{15}NO_2SNa$ 200.0721, Obtained 200.0728.

Preparation of 2

To an ice cooled solution of **1** (400 mg, 2.2 mmols) in 1:1 CH_3CN/1N NaOH, pH=10, Boc anhydride (738 mg, 3.3 mmols) was added over a period of 1 h at regular interval of time. After stirring for 12 h, solvent was evaporated, diluted with water, and acidified with aq. $KHSO_4$ solution to pH=2. It was then extracted with ethtyl acetate, dried over Na_2SO_4, evaporated and recrystallized from acetone.

%Yield: 82%

m.p : 280-282°C

^{1}H NMR (D_2O, 300 MHz) δ: 1.11 (s, 18H), 2.93 (br dd, 2H), 3.85 (m, 1H)

^{13}C NMR (D_2O,75 MHz) δ: 26.4, 29.3, 32.4, 42.1, 56.8, 80.1, 155.3, 172.3

IR (KBr): 3374, 1732, 1687, 1518, 1460, 1445, 1417, 1392, 1368, 1343, 1285 cm^{-1}.

HRMS : Calculated for $C_{12}H_{23}NO_4SK$ 316.0985, Obtained 316.0981.

Preparation of 3a

To an ice cooled solution of S-*tert*butyl Boc-Cysteine (200 mg, 0.72 mmol) in dry CH_2Cl_2; was added N-hydroxysuccinimide (NHS) (99 mg, 0.86 mmol) and dicyclohexycarbodiimide (DCC) (177 mg, 0.86 mmol). After 5 minutes, 1-Pyrenemethylaminehydrochloride (230 mg, 0.86 mmol) and triethylamine (0.12 mL, 0.86 mmol) were added and the reaction mixture was stirred for 24 h. Reaction mixture was filtered and the filtrate was washed sequentialy with 0.2N H_2SO_4, aq. $NaHCO_3$ solution and finally with water. The organic layer was dried over Na_2SO_4, evaporated and purified by column chromatography using ethyl acetate and hexane as eluents to yield 170 mg of the compound.

%Yield: 48%

m.p : 180-182^{o}C

^{1}H NMR ($CDCl_3$, 300 MHz) δ: 1.37 (s, 9H), 1.54 (s, 9H), 2.88 (br s, 2H), 4.82 (m, 2H), 5.23 (br m, 1H), 5.41 (d, *J* = 9.3 Hz, 1H), 7.82-8.10 (m, 9H)

^{13}C NMR ($CDCl_3$,75 MHz) δ : 28.1, 30.6, 30.7, 42.7, 47.3, 54.1, 80.1, 122.8,123.3, 124.6, 125.0, 125.3, 125.9, 127.1, 127.4, 127.5, 128.1, 128.3, 129.1, 130.5, 130.7, 131.0, 131.3, 155.3, 170.3,

IR (KBr) : 3325, 3039, 2926, 2851, 1689, 1628, 1575, 1532, 1440, 1367, 1312 cm^{-1}.

HRMS : Calculated for $C_{29}H_{35}N_2O_3S$ 491.2368, Obtained 491.2366.

Preparation of 3b

To an ice cooled solution of S-*tert*butyl Boc-Cysteine (200 mg, 0.72 mmol) in dry CH_2Cl_2; (NHS) (99 mg, 0.86 mmol); (DCC) (177 mg, 0.86 mmol) were added. After 5 minutes, L-tryptophanmethylesterhydrochloride (218 mg, 0.86 mmol) and triethylamine (0.12 mL, 0.86 mmol) were added and reaction was stirred for 24 h. Reaction mixture was filtered and the

CH_2Cl_2 layer was washed sequentialy with 0.2N H_2SO_4, $NaHCO_3$ solution and finally with water. The filtrate was dried over Na_2SO_4, evaporated and purified by column chromatography using ethyl acetate and hexane as eluents to yield 170 mg of the compound.

%Yield: 50%

m.p : 220^{o}C

^{1}H NMR (CD_3CN, 300 MHz) δ: 1. 28 (s, 9H), 1.40 (s, 9H), 2.81 (br dd+dd, 2H), 3.16 (d, *J* = 6.6 Hz, 2H), 3.63 (s, 3H), 4.15 (m, 1H), 4.72 (q, *J* = 6 Hz, 1H), 5.61 (m, 1H), 7.04-7.16 (m, 4H), 7.40 (d, *J* = 7.8 Hz, 1H), 7.53 (d, *J* = 7.5 Hz, 1H), 9.27 (br s, 1H)

^{13}C NMR (CD_3CN,75 MHz) δ : 28.1, 28.5, 31.1, 31.3, 43.0, 52.8, 54.1, 55.5, 80.3, 110.3, 112.4, 119.3, 120.0, 122.6, 124.8, 128.4, 137.3, 156.3, 171.4, 172.8

IR (KBr) : 3330 (br), 2977, 2927, 1666 (br), 1517 (br), 1449, 1366, 1248, 1165, 1049 cm^{-1}

HRMS : Calculated for $C_{24}H_{36}N_3O_5S$ 478.2376, Obtained 478.2374.

Metal ion binding studies using UV-Visible spectroscopy

Stock solutions of compounds **3a** and **3b** with a concentration of 10^{-5} M were made in acetonitrile. Stock solutions of metal perchlorates (10^{-4} M) were made in acetonitrile. The metal ion were titrated against compounds **3a** and **3b**. The absorption spectra were recorded using Shimadzu double beam spectrophotometer, UV-2400. The titration was continued till a saturation point was observed.

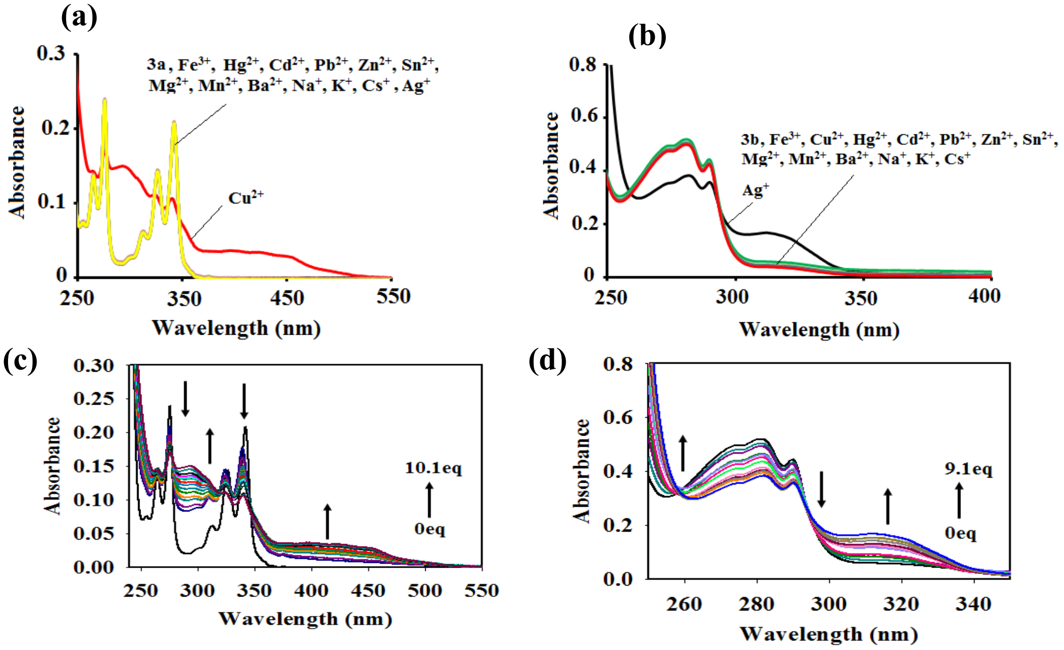

Figure S1: (a) UV-Visible spectra for **3a** with and without metal ions in CH_3CN. Cu^{2+} ions 10 equiv and other metal ions 50 equiv (b) UV-Visible spectra for **3b** with and without metal ions in CH_3CN. Ag^+ ions 10 equiv and other metal ions 50 equiv. (c) UV-visible spectra of **3a** alone and with the addition of $Cu(ClO_4)_2$ in CH_3CN. (d) UV-visible spectra of **3b** upon the addition of $AgClO_4$ in CH_3CN.

Metal ion binding studies using fluorescence spectroscopy

Stock solutions of compounds **3a** and **3b** with a concentration of 10^{-5} M were made in acetonitrile. Stock solutions of metal perchlorates (10^{-4} M) were made in acetonitrile. The compounds were titrated against the metal ions and the emission spectra were recorded using

HORIBA JOBIN YVON Scientific, fluoromax - 4 spectrofluorometer with slit width of 5 nm. The titration was continued till a saturation point was observed.

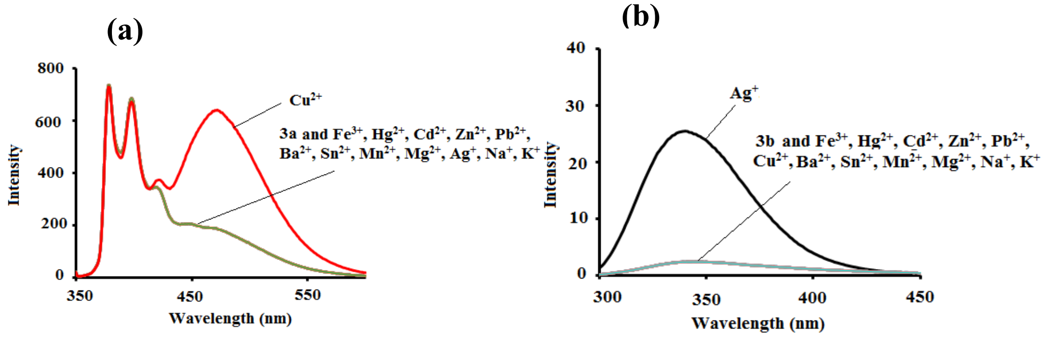

Figure S2: (a) Fluorescence spectral studies of **3a** with various metal ions in CH_3CN, the results obtained are for 5 equiv of Cu^{2+} and for 55 equiv of other metal ions, $\lambda_{exc} = 340$ nm (b) Fluorescence spectral studies of **3b** in CH_3CN, 50 equiv other metal ions and 3 equiv of Ag^{+}, $\lambda_{exc} = 290$ nm.

ESI-HRMS showing the 2:1 complex of 3a with Cu^{2+} and 1:2 complex of 3b with Ag^{+}

Compound **3a** (500 μM) and $Cu(ClO_4)_2$ (500 μM) solutions were made in CH_3CN and 5 equivalents of $Cu(ClO_4)_2$ solution was added to **3a** and the resulting solution was analyzed by ESI mass spectrometry. Compound **3b** (500 μM) and $AgClO_4$ (500 μM) solutions were made in CH_3CN and 5 equivalents of $AgClO_4$ solution was added to **3b** and the resulting solution was analyzed by ESI mass spectrometry.

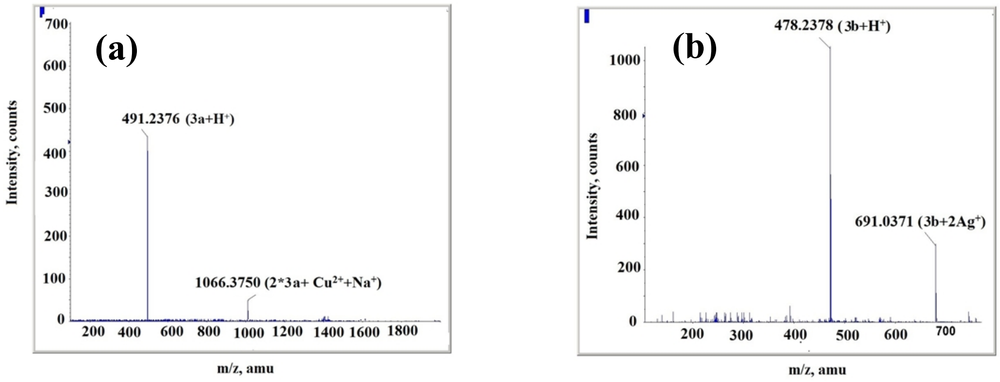

Figure S3: ESI-HRMS of (a) **3a**-Cu(II) complex (b) **3b**-Ag(I) complex.

Determination of stoichiometry of complex

A series of solutions containing compounds (**3a**, **3b**) (10^{-5} M) and metal ions (10^{-5} M) were prepared in CH_3CN. The molefraction of the receptors were varied from 0.1 to 1 and the changes in absorbance after correction factor were plotted against the molefraction.

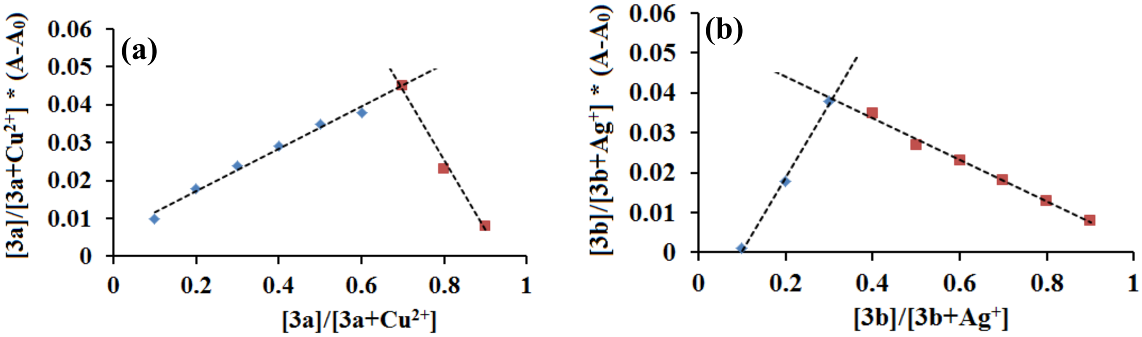

Figure S4: Job's plot of (a) **3a** with Cu^{2+} (b) **3b** with Ag^+

Ecxiation spectra

Excitation spectra was recorded on a steady-state fluorescence spectrophotometer with a slitwidth of 5 nm. The redshift in emission intensity indicates the static type excimerr formation in **3a-**Cu^{2+}.

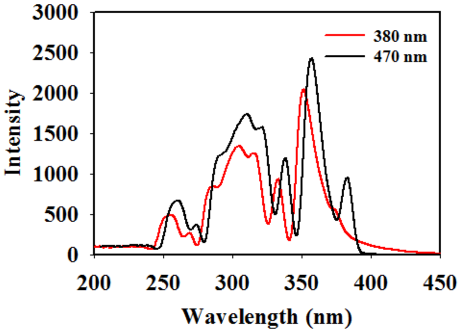

Figure S5: Excitation spectra for **3a** with 5 equiv of Cu^{2+} in CH_3CN.

Time-resolved fluorescence data for 3a and 3b with metal ions

Time-resolved fluorescence experiments were performed by using an IBH picosecond single photon-counting system employing an adjustable nano-LED excitation source and a Hamamatsu

C4878-02 micro channel plate (MCP) detector with a slit width of 5 nm. Data were collected at room temperature with a 4 mm optical path fluorescence cell filled with the solutions of compounds in acetonitrile. The decay time was calculated by the linear least square fit method and single exponetial fit was observed for Trp excitation at 290 nm and double exponential fit for Pyrene excitation at 340 nm. Both compounds and metal ions were prepared in CH_3CN with a concentration of 10^{-5} M.

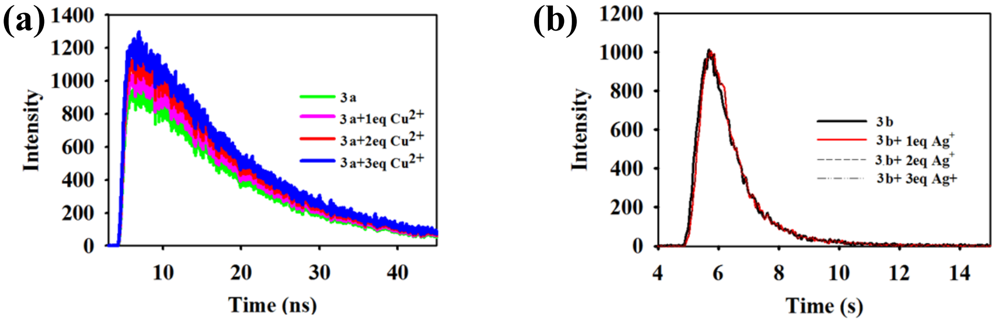

Figure S6: Time-resolved fluorescence spectra of (a) **3a** upon adding various equivalents of Cu^{2+} , λ_{exc} = 340 nm, collection at 470 nm (b) **3b** with various equivalents of Ag^{+}, λ_{exc} = 290 nm, collection at 330 nm.

Table S1: Parameters calculated from time-resolved fluorescence spectra of **3a** alone and **3a** with Cu^{2+}.

Compounds	λ_{exc}	$\lambda_{collection}$	τ_1 **(ns)**	τ_2 **(ns)**	A_1	A_2	χ^2
3a	340 nm	470 nm	3.11	14.09	6.92	93.08	1.01
3a +1 equiv Cu(II)	340 nm	470 nm	3.14	14.01	17.71	82.29	1.06
3a + 2 equiv Cu(II)	340 nm	470 nm	3.10	14.01	13.23	86.77	1.03
3a + 3 equiv Cu(II)	340 nm	470 nm	3.15	14.03	12.92	87.08	1.11

Table S2: Parameters calculated from time- resolved fluorescence spectra of **3b** alone and **3b** with Ag^+.

Compound	λ_{exc}	$\lambda_{collection}$	τ	A_1
3b	290 nm	330 nm	1.01	100
3b +1 equiv Ag(I)	290 nm	330 nm	0.99	100
3b+ 2 equiv Ag(I)	290 nm	330 nm	1.0	100
3b+ 3equiv Ag(I)	290 nm	330 nm	1.01	100

Competitive metal ion binding by fluorescence spectroscopy

An equimolar solutions of **3a** and **3b** (10^{-5} M) and metal ions (10^{-4} M) were prepared in CH_3CN. The emission intensities of the molecules (**3a** and **3b**) with (I) and without (I_0) metal ions were recorded with steady-state fluorescence. The response towards metal ion obtained by plotting the change in emission intensity ($I-I_0$) against the metal ions

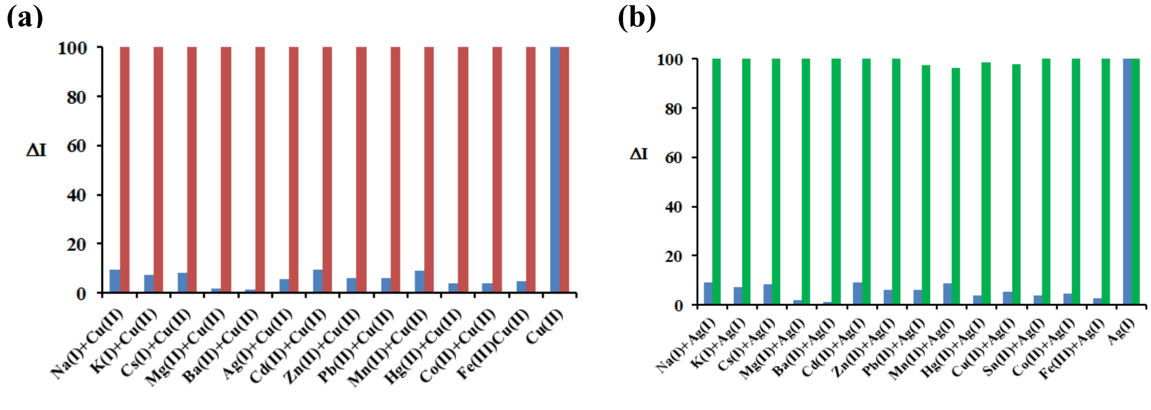

Figure S7: Competitive binding studies of (a) **3a** (b) **3b** towards various metal ions. The binding was studied by steady-state fluorescence spectroscopic analysis.

Determination of binding constant

The binding constant (K_{21}) for 2:1 binding of compound **3a** with Cu^{2+} was determined by equation 1.

$$2H+G \rightleftharpoons GH_2$$

$$[G]_{tot} = \frac{a}{2K_{21}(1-a)^2[H]_{tot}} + \frac{a[H]_{tot}}{2} \qquad (1)$$

[H_{tot}] and [G_{tot}] denote the total concentrations of **3a** and Cu^{2+}, and the term *a* is the ratio of change in absorbance ratio ie. $(A- A_0)/(A_i - A_0)$, where *A* is the absorbance at added metal ion, and A_0 and A_i are the intensity at zero and infinite cation concentrations.

The association constant of **3b** with Ag^+ was determined UV-Visible spectroscopically by employing Benesi-Hildebrand method.

$$1/ A_0\text{-}A = 1/(A_0\text{-}A_\infty)K[G]^2 + 1/(A_0\text{-}A_\infty)$$

Where A and A_0 are the absorbance intensities of **3b** with and without Ag^+ and A_∞ is the absorbance intensity for infinite dilution of **3b** with Ag^+.

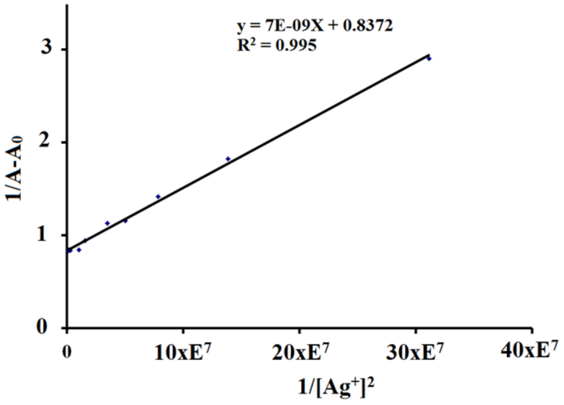

Figure S8: Benesi-Hildebrand plot for **3b** with Ag^+.

ITC experiments on complexation

The thermodynamic parameters were determined by using MicroCal iTC$_{200}$ system at 298K in acetonitrile. Sample solution (**3a**) of 200 μM was taken in the cell and 30 μM of Cu(ClO$_4$)$_2$ was slowly added. Roughly 4equiv of titrant was added to sample solution. The nonlinear least square algorithm was used to determine the best fit values for change in enthalpy (ΔH) and binding constant (K). Similarly, sample solution (**3b**) of 150 μM was taken in the cell and 50 μM of AgClO$_4$ was slowly added.

Table S3. ITC studies on the complexation of **3a** and **3b** toward Cu^{+2} and Ag^{+}.

Binding between	**K (M^{-1})**	**ΔG$_1$ (KJ/mol)**	**ΔH$_1$ (KJ/mol)**	**TΔS$_1$ (KJ/mol)**
3a and Cu^{2+}	1.95x10^5	-30.18	-19.13	11.05

Binding between	**K$_1$ (M^{-1}) and K$_2$ (M^{-1})**	**ΔG$_1$ (KJ/mol) and ΔG$_2$ (KJ/mol)**	**ΔH$_1$ (KJ/mol) and ΔH$_2$ (KJ/mol)**	**TΔS$_1$ (KJ/mol) and TΔS$_1$ (KJ/mol)**
3b and Ag$^+$	1.95x10^5; 1.97x10^8	-30.18; -47.32	-19.13; -70.53	11.05; -23.21

SEM and AFM analysis of 3a and 3b

The compounds **3a** and **3b** were dissolved in CH$_3$CN in order to get a 1 mM solution. The metal salts Cu (ClO$_4$)$_2$ and AgClO$_4$ were prepared in CH$_3$CN and mix with **3a** and **3b** respectively such that 3 equiv of metal ions were present in the solution. All the sample solutions were drop-casted on a carbon tape, pasted on a stub, dried at room temperature and coated with ~10 nm of gold. Images were recorded by ZEISS EVO®18 instrument with an EHT of 20 kv.

Similar solutions were drop-casted on silicone wafer and samples were recorded using Nanoscope Multimode AFM operating at tapping mode in air. The images were taken in the air at room temperature and data analysis were performed using Nanoscope 5.31r1 software.

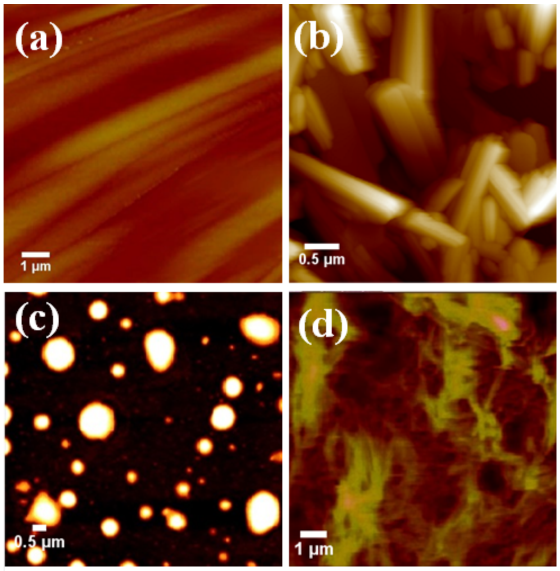

Figure S9: AFM images of (a) **3a** (b) **3a**+Cu^{2+} (c) **3b** (d) **3b**+Ag^{+}.

Density functional theory (DFT) calculation

The DFT calculations were done using the Guassian 09 suite of programs.[1] The binding modes of **3a** with Cu^{2+} and **3b** with Ag^{+} was investigated by (unrestricted) UB3LYP/6-31G(d) level of density functional theory (DFT) and B3LYP/Gen1 level of DFT, respectively , where Gen1 corresponds to 6-31G(d) basis set for H, C, N, O and S atoms and LanL2DZ basis set with 'f' polarization function for Ag atom.

The NMR calculations were performed by GIAO method from the coordinates of the optimised structures of the uncomplexed and complexed systems.

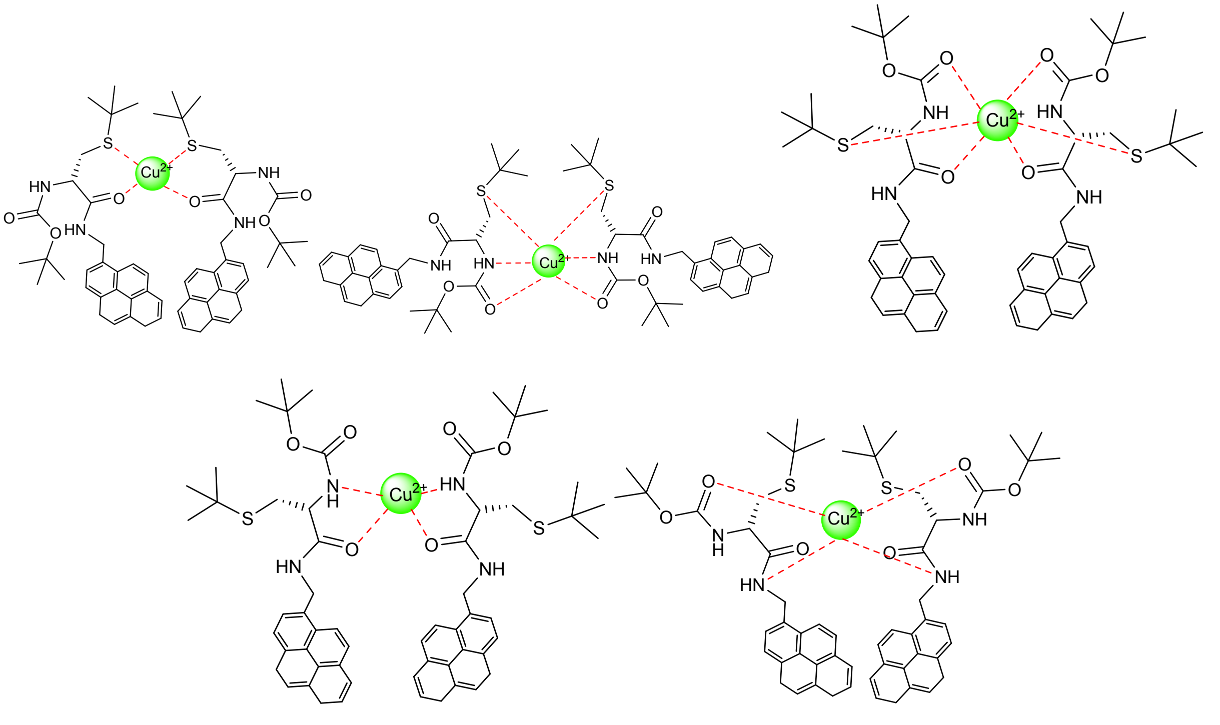

Figure S10. Possible binding modes of Cu^{2+} with **3a**. Initial structures resembling to these configurations are subjected to DFT level optimization.

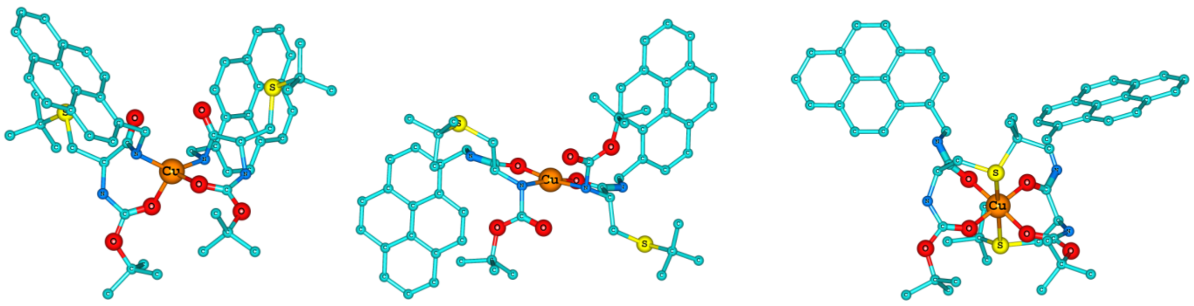

$E_{rel} = 32.4$

$E_{rel} = 5.4$

$E_{rel} = 0.0$

Figure S11. Final Optimized structures of Cu^{2+} complex of **3a** obtained by DFT calculation. The relative energy (E_{rel}) in kcal/mol is also shown below each structure. UB3LYP/6-31G* level theory was used for the computation.

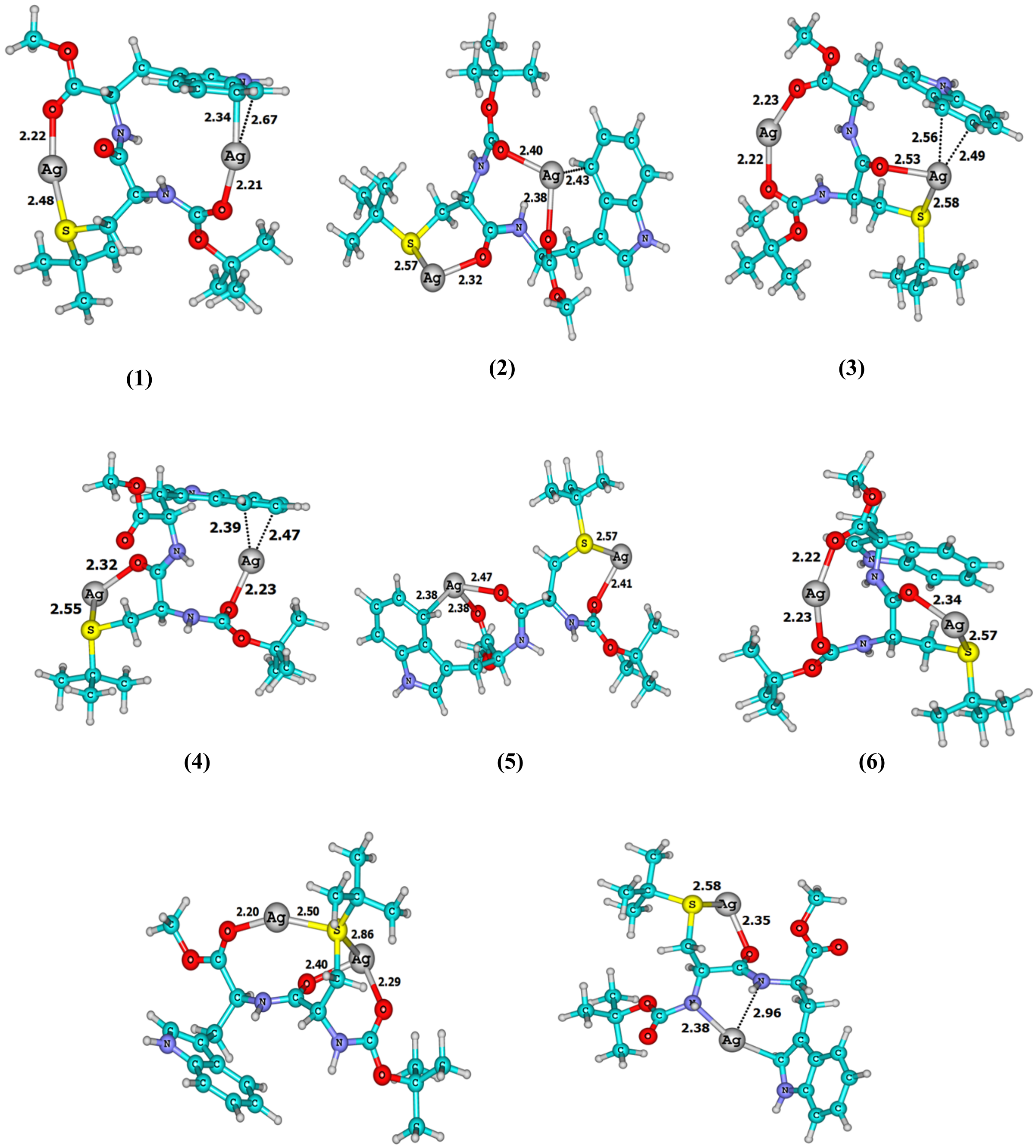

(1) **(2)** **(3)**

(4) **(5)** **(6)**

(7) **(8)**

Figure S12. The optimized structures of eight different possible binding modes (**1-8**) in the decreasing order of stability for **3b**–Ag$^+$ complex. The level of theory used is B3LYP/Gen1. Gen1 corresponds to 6-31G(d) basis set for H, C, N, O and S atoms and LanL2DZ basis set with 'f' polarization function for Ag atom.

Table S4. The relative order of stability in kcal/mol for **1-8** complexes. For the structures of **1-8**, please see Figure S12

Complex	Relative. Energy (kcal/mol)
1	0.0
2	8.8
3	9.3
4	13.9
5	14.3
6	14.8
7	16.1
8	33.9

NMR Titraton Experiments

The involvement of indole moiety in metal ion binding was confirmed by ^{13}C NMR in CD_3CN. A solution of **3b** (600 μM) in CD_3CN was prepared and ^{13}C NMR was recorded. **3b** was added to a solution of $AgClO_4$ in CD_3CN **(**600 μM**)** and ^{13}C NMR was recorded. Similar solutions were used for ^1H NMR titrations also.

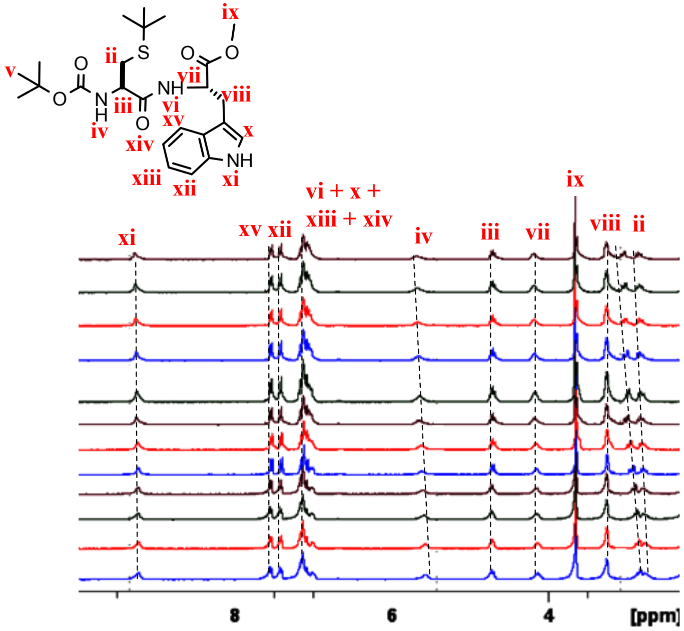

Figure S13: ^1H NMR (300 MHz, CD_3CN) spectra of **3b** alone and with the addition of $AgClO_4$ (0-10 euiv). The lower NMR trace represents **3b** alone and the the remaining spectra from down to up represent the increasing amounts of $AgClO_4$.

Table S5. Theoretically calculated ^{13}C NMR chemicalshifts for **3b** and **3b**+Ag^{+}. The highlight indicates the shift ($\Delta\delta$) expected for **3b** . 2Ag^{+} complex. The experimental spectral data are given for comparison. The convergence of experimental and theoretical values are clear from the table.

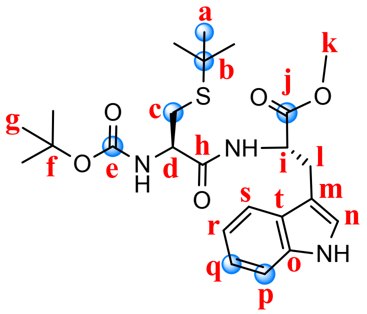

System	Experimental ^{13}C NMR values (ppm)			Calculated ^{13}C NMR values by DFT (ppm)		
C-atoms	**3b**	**3b**+Ag^{+}	$\Delta\delta$	**3b**	**3b**+A^{+}	$\Delta\delta$
a	31.13	31.44	0.31	30.81	31.11	0.29
b	42.98	43.80	0.82	36.34	37.12	0.77
c	31.31	31.48	0.17	30.71	30.81	0.10
d	55.52	55.52	0.0	53.34	53.34	0.0
e	156.28	156.83	0.55	158.23	158.81	0.57
f	80.31	80.31	0.0	60.88	60.91	0.02
g	28.48	28.49	0.01	27.49	27.49	0.0
h	171.41	171.41	0.0	172.04	172.05	0.01
i	54.09	54.09	0.0	56.92	56.93	0.01
j	172.84	173.42	0.58	172.98	173.62	0.63
k	52.75	52.75	0.0	56.92	56.93	0.01
l	28.10	28.11	0.01	28.99	28.99	0.0
m	110.30	110.30	0.0	107.53	107.53	0.0
n	124.75	124.75	0.0	127.28	127.31	0.02
o	137.34	137.34	0.0	140.07	140.08	0.01
p	112.38	112.85	0.47	113.62	114.01	0.38
q	119.26	119.47	0.21	117.69	117.91	0.21
r	120.04	120.04	0.0	124.32	124.33	0.01
s	122.56	122.56	0.0	119.90	119.91	0.01
t	128.44	128.44	0.0	127.25	127.26	0.01

Reference.

1. Frisch, M. J.; Trucks, G. W.; Schlegel, H. B.; Scuseria, G. E.; Robb, M. A.; Cheeseman, J. R.; Scalmani, G.; Barone, V.; Mennucci, B.; Petersson, G. A.; Nakatsuji, H.; Caricato, M.; Li, X.; Hratchian, H. P.; Izmaylov, A. F.; Bloino, J.; Zheng, G.; Sonnenberg, J. L.; Hada, M.; Ehara, M.; Toyota, K.; Fukuda, R.; Hasegawa, J.; Ishida, M.; Nakajima, T.; Honda, Y.; Kitao, O.; Nakai, H.; Vreven, T.; Montgomery, J., J. A.; Peralta, J. E.; Ogliaro, F.; Bearpark, M.; Heyd, J. J.; Brothers, E.; Kudin, K. N.; Staroverov, V. N.; Keith, T.; Kobayashi, R.; Normand, J.; Raghavachari, K.; Rendell, A.; Burant, J. C.; Iyengar, S. S.; Tomasi, J.; Cossi, M.; Rega, N.; Millam, J. M.; Klene, M.; Knox, J. E.; Cross, J. B.; Bakken, V.; Adamo, C.; Jaramillo, J.; Gomperts, R.; Stratmann, R. E.; Yazyev, O.; Austin, A. J.; Cammi, R.; Pomelli, C.; Ochterski, J. W.; Martin, R. L.; Morokuma, K.; Zakrzewski, V. G.; Voth, G. A.; Salvador, P.; Dannenberg, J. J.; Dapprich, S.; Daniels, A. D.; Farkas, O.; Foresman, J. B.; Ortiz, J. V.; Cioslowski, J.; Fox, D. J. Gaussian 09, Revision C.01, 2010.

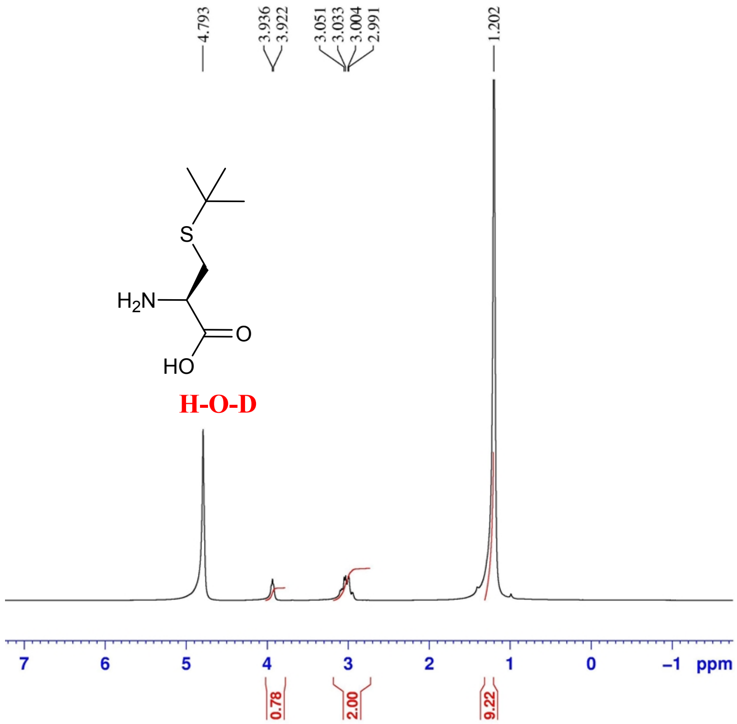

^{1}H NMR spectrum of **1** in D_2O (300MHz)

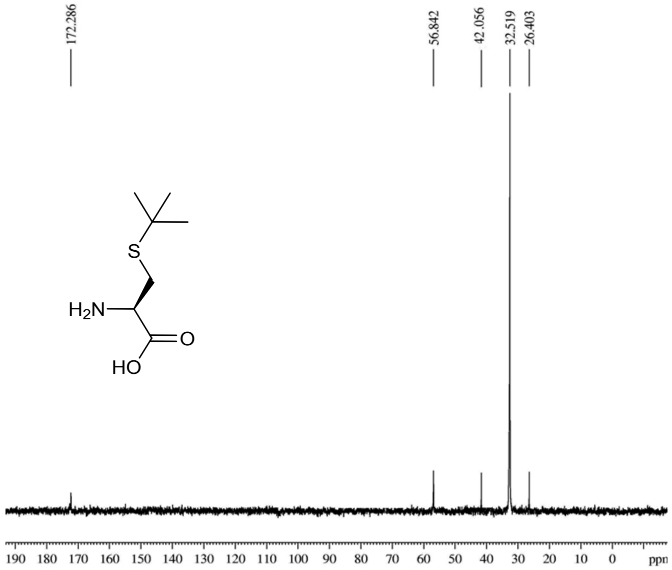

^{13}C NMR spectrum of **1** in D_2O (75MHz)

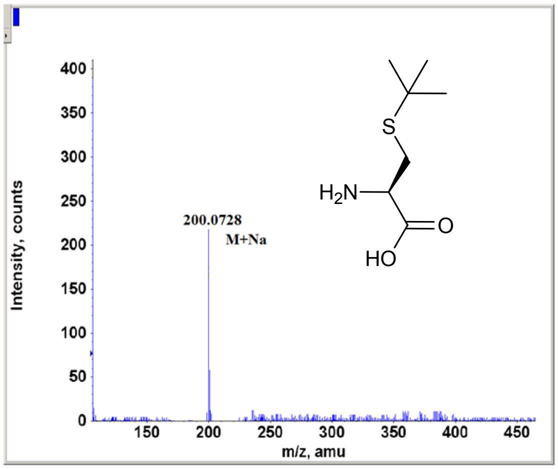

ESI-Mass spectrum of **1**

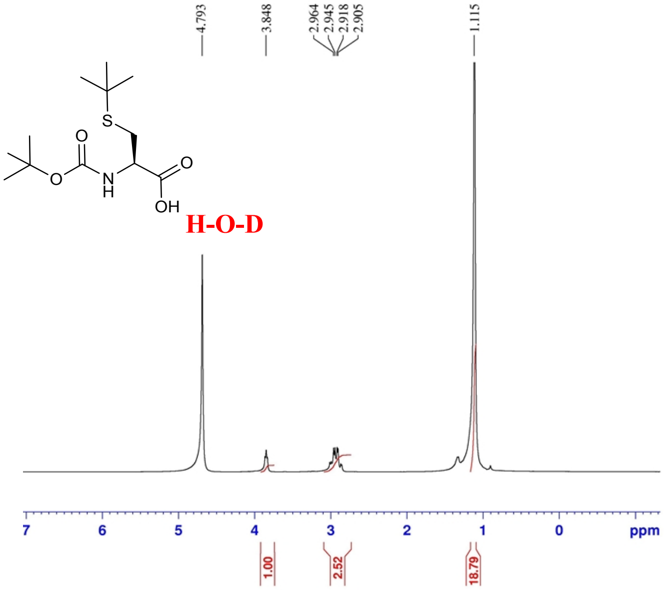

^{1}H NMR spectrum of **2** in D_2O (300MHz)

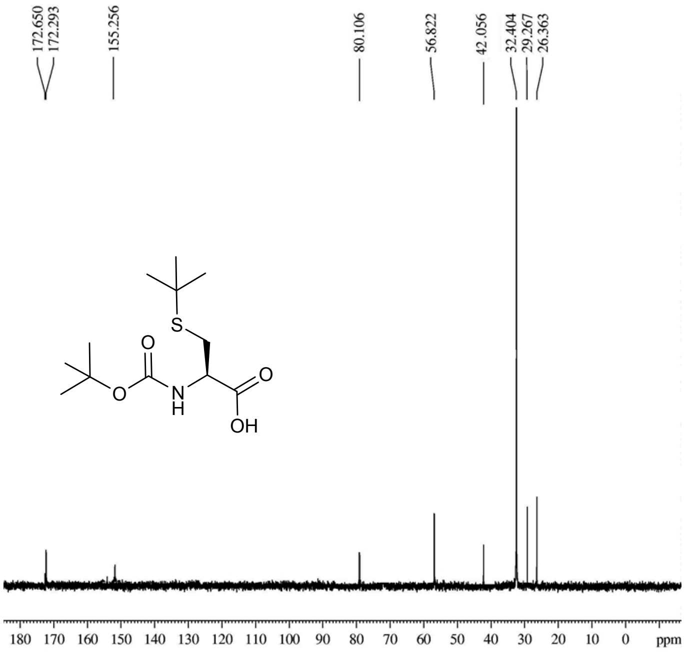

^{13}C NMR spectrum of **2** in D_2O (75MHz)

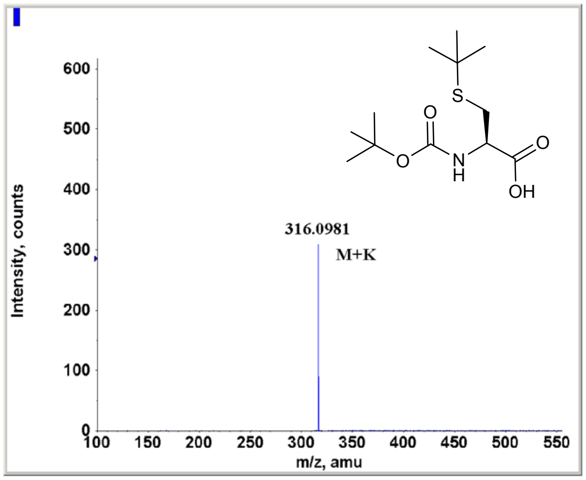

ESI-Mass spectrum of **2**

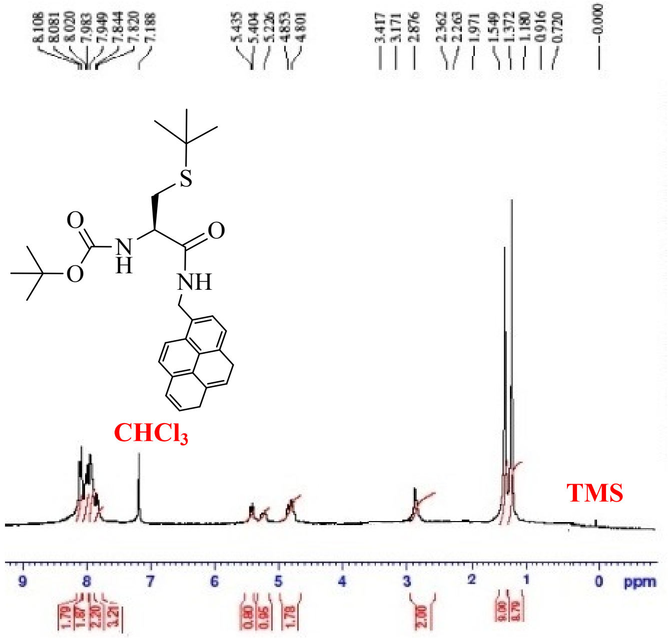

^{1}H NMR spectrum of **3a** in $CDCl_3$ (300MHz)

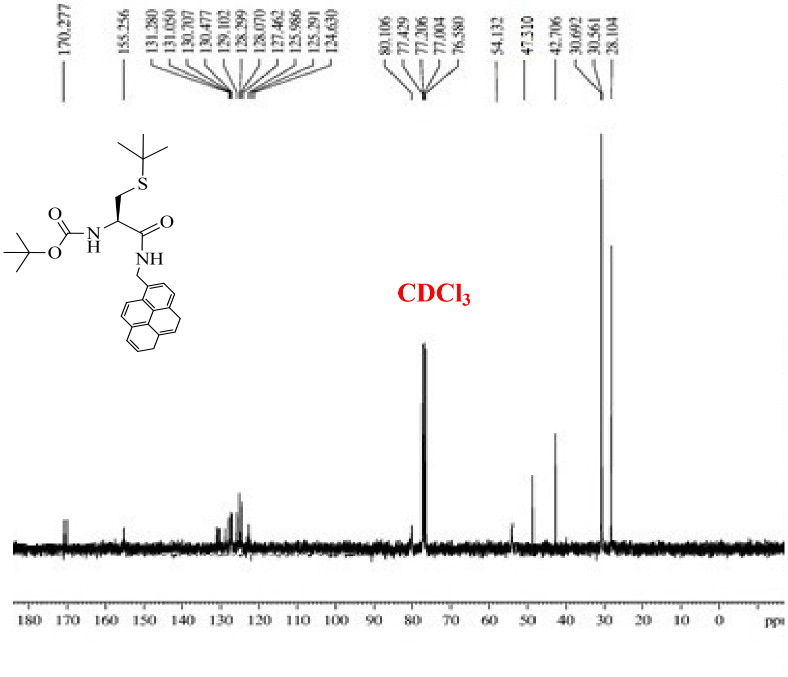

^{13}C NMR spectrum of **3a** in $CDCl_3$ (75MHz)

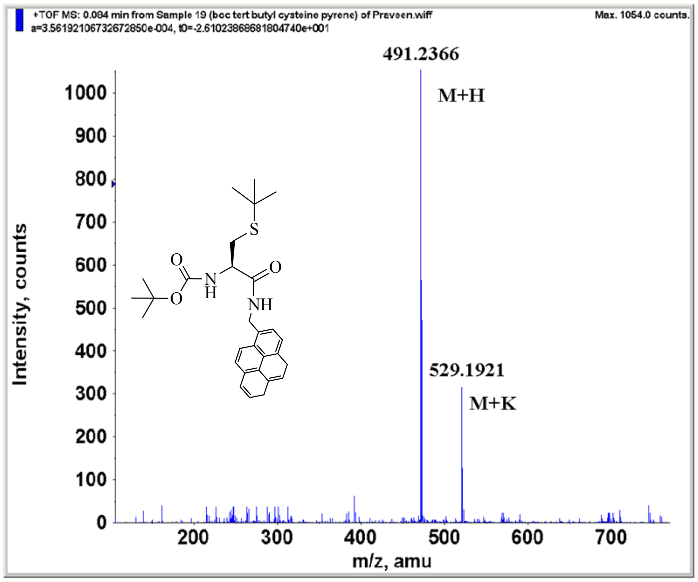

ESI-Mass spectrum of **3a**

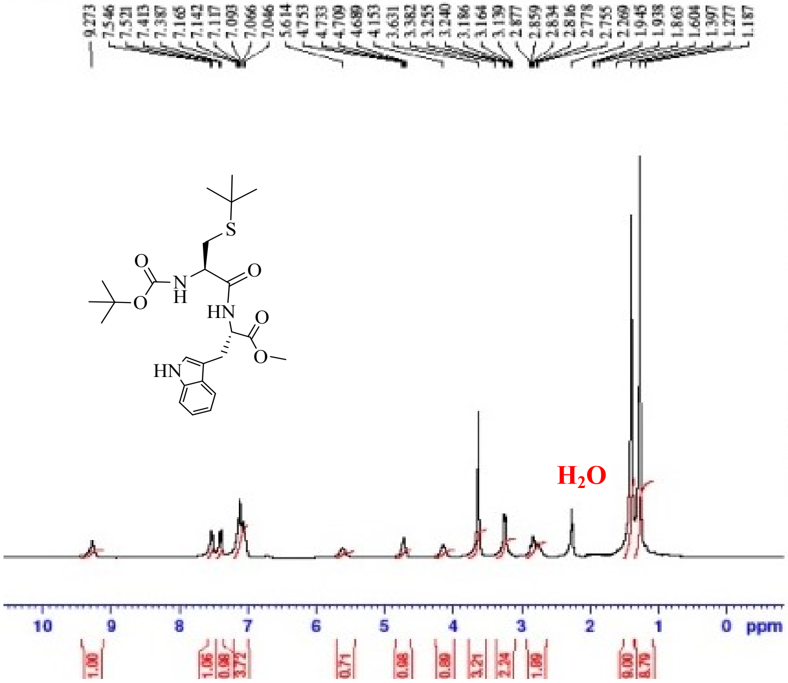

^{1}H NMR spectrum of **3b** in CD_3CN (300MHz)

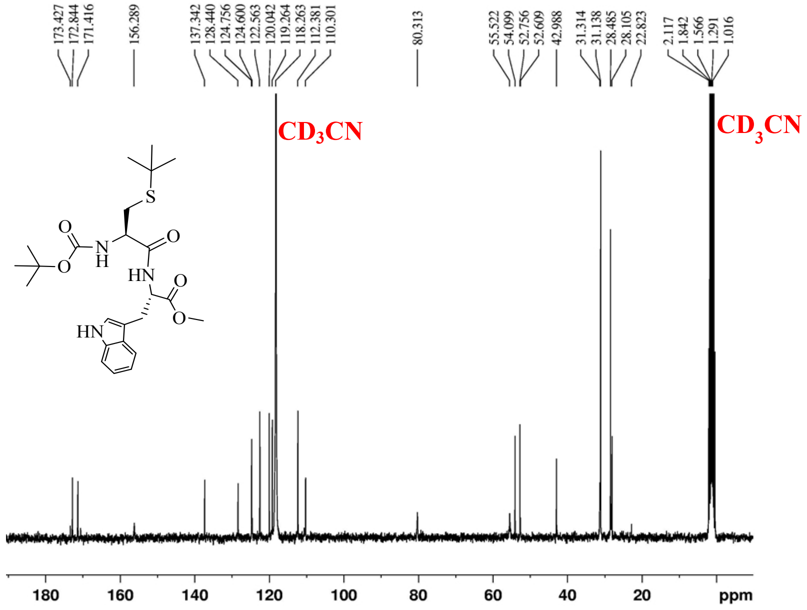

^{13}C NMR spectrum of **3b** in CD_3CN (75MHz)

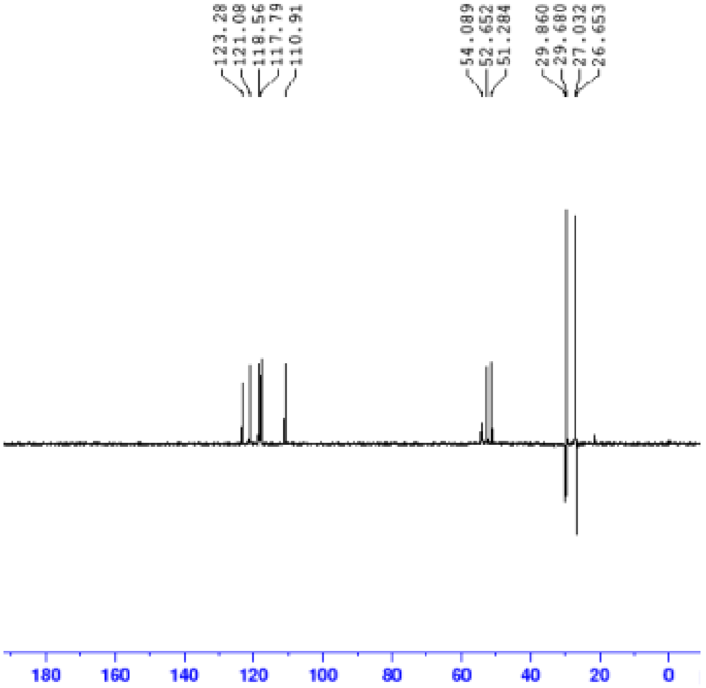

DEPT-135 NMR spectrum of **3b** in CD_3CN (75MHz)

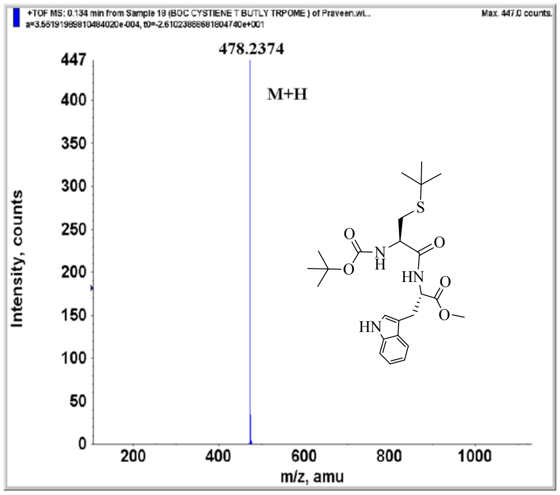

ESI-Mass spectrum of **3b**